Review

Functional porous carbon-based composite electrode materials for lithium secondary batteries

Kai Zhang,   Zhe Hu,   Jun Chen*

Key Laboratory of Advanced Energy Materials Chemistry (Ministry of Education), Chemistry College, Nankai University, Tianjin 300071, China
[Manuscript received November 7, 2012; revised March 26, 2013]

Abstract

The synthetic routes of porous carbons and the applications of the functional porous carbon-based composite electrode materials for lithium secondary batteries are reviewed. The synthetic methods have made great breakthroughs to control the pore size and volume, wall thickness, surface area, and connectivity of porous carbons, which result in the development of functional porous carbon-based composite electrode materials. The effects of porous carbons on the electrochemical properties are further discussed. The porous carbons as ideal matrixes to incorporate active materials make a great improvement on the electrochemical properties because of high surface area and pore volume, excellent electronic conductivity, and strong adsorption capacity. Large numbers of the composite electrode materials have been used for the devices of electrochemical energy conversion and storage, such as lithium-ion batteries (LIBs), Li-S batteries, and Li-O$_2$ batteries. It is believed that functional porous carbon-based composite electrode materials will continuously contribute to the field of lithium secondary batteries.

Key words

porous carbons; functional materials; composite electrode materials; synthetic method; lithium secondary batteries
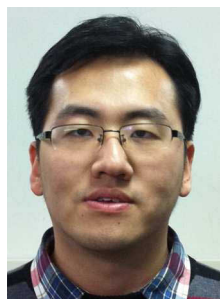
Kai Zhang received his BS degree in material chemistry from Nankai University (2010) and then joined the Key Laboratory of Advanced Energy Materials Chemistry to study for his PhD under the supervision of Prof. Jun Chen. His research focuses on polyanion-type cathode materials and porous carbons for rechargeable batteries.

Jun Chen is a Cheung Kong Scholar Professor and Chief Scientist of the National Nano Key Science Research. He is the director of the Key Laboratory of Advanced Energy Materials Chemistry (Ministry of Education) at Nankai University. He leads a team focused on nanomaterial electrochemistry and high-energy batteries. He was awarded the National Natural Science Award (2nd prize) in 2011. His research expertise is energy conversion and storage with batteries, fuel cells and solar cells.

Zhe Hu received his BS degree in chemistry from Nankai University (2011) and then joined the Key Laboratory of Advanced Energy Materials Chemistry to study for his master's degree under the supervision of Prof. Jun Chen. His research focuses on polyanion-type cathode materials for rechargeable Li ion batteries.

1. Introduction

Carbon, which is located in the IV main group of the second period in the periodic table, has been widely used in the fields of chemical industry, electronic devices, and electrochemical energy storage and conversion [1−4]. Via sp^3 and sp^2 covalence linkages, considerable allotropes such as diamond, graphite, graphene, fullerene, carbon nanotube, and amorphous carbon can be formed. Among them, an application form is porous carbon with outstanding physical and chemical properties [5–8]. According to the pore size, porous carbons are classified into three categories: micropores (<2 nm), mesopores (2–50 nm), and macropores (>50 nm). Porous carbons, which are usually obtained via carbonization and activation of natural or synthetic precursors, have been applied to the areas of gas adsorption, catalytic reaction, chromatographic separation, batteries, and fuel cells [9−11].

In the field of electrochemical energy storage and conversion, porous carbon materials are extensively applied to lithium-ion batteries (LIBs), metal-air batteries, hydrogen-oxygen fuel cells, and electrochemical supercapacitors (Figure 1) because of their excellent electronic conductivity, large specific surface area, favorable chemical stability, and low-cost. Some conductive agents such as Vulcan XC-72 [12] and Super P [13] are porous carbons. The conductive agents ameliorate electronic transport among the electrode materials to improve the electrochemical performance of the batteries. Furthermore, porous carbons are also used as anode materials of lithium ion batteries, oxygen reduction reaction (ORR) catalysts, and electrode materials of electrochemical capacitors. Recently, the functional porous carbon-based composite materials for lithium secondary batteries have attracted great interests for the possibility to overcome many disadvantages including low electronic conductivity, large volume expansion, and dissolution in the electrolyte. This combination results in obtaining high energy density of the batteries. The composite electrodes show excellent high-rate performance, long cycling stability, and high catalytic properties. Therefore, we here review the most recent and important scientific progresses of functional porous carbon-based composite electrode materials. In particular, the synthetic methods of porous carbons and the effects of porous carbons on the composite electrode properties for lithium secondary batteries have been focused on.
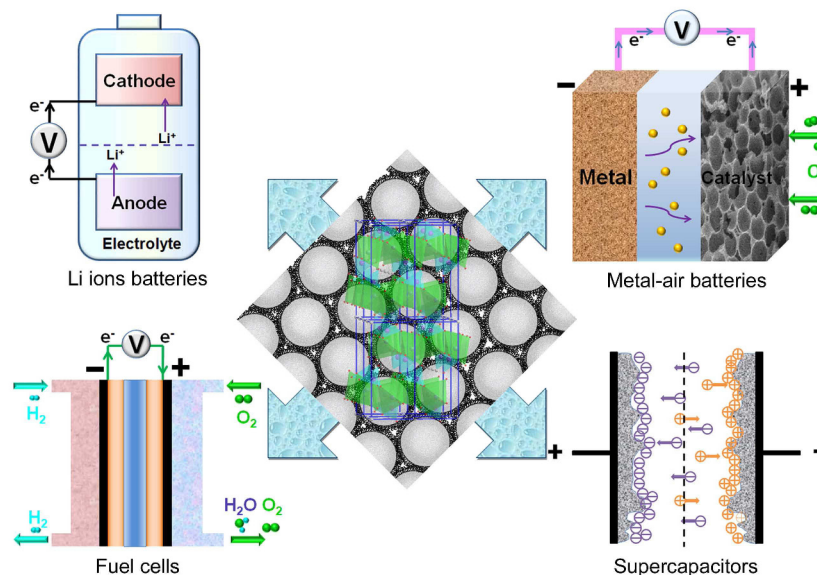

Figure 1. Representative applications of porous carbons in the field of electrochemical energy conversion and storage (Li-ion batteries, metal-air batteries, fuel cells, and supercapacitors)

2. Preparation of porous carbons

In the past few decades, various synthetic methods including template method [14] and activation process [15] were developed to fabricate porous carbons. Template method has been used to synthesize all kinds of porous carbon materials. While, the activation process is usually adopted to prepare microporous activated carbons.

2.1. Template method

The template method includes hard-template process and soft-template process. The hard templates refer to presynthesized organic or inorganic templates, while soft templates are self-assembled templates which are synthesized by the self-assembly of organic templates [9]. The hard-template process of porous carbon includes the synthesis of templates, soakage of the template in a suitable carbon precursor, carbonization of the precursor, and subsequent removal of the template. The soft-template process does not need the preparation of templates beforehand.

2.1.1. Hard-template process

The hard templates mainly serve as matrix for replication of porous carbon materials. The porous structures are designed by the nanostructures of templates, so the synthesis of the template material with connected three-dimensional porous structure is essential.

Ordered microporous carbon materials can be synthesized by using zeolites as templates. Kyotani et al. [16,17] used zeolite Y as a template to synthesize ordered microporous carbon with high surface area (3600 $m^2 \cdot g^{-1}$) and highly ordered structure. Ordered mesoporous carbon materials have been synthesized using molecular sieves as templates. Ryoo and co-workers developed a new mesoporous carbon (CMK-3) which was the first to retain the structural symmetry for ordered mesoporous silica template (SBA-15) [18]. To improve the electronic conductivity of ordered mesoporous carbon, the strategies with fused aromatic precursors as carbon source, chemical vapor deposition (CVD) at high temperature (> 900 °C), and carbonization over 2000 °C to cause a graphitization process have been used [19,20].

A variety of templates such as silica nanoparticles, anodic alumina, and silica gel have been developed for the synthesis of disordered mesoporous carbon materials [21−23]. Kyotani et al. [23,24] developed carbon nanotubes (CNTs) and submicro-tubes in 1D channels using an AAO film as a template.

Siliceous opals are natural templates, which are prepared by self-assembly of SiO_2 spheres. Zakhidov et al. [25] used porous silica opal template to prepare ordered macroporous carbons that were three-dimensionally periodic on the scale of optical wavelengths. In comparison, biological materials contain both organic and inorganic component. The organic component (fiber) provides the carbon source for porous carbon materials; while the inorganic component (apatite) is well-dispersed in the organic component in a specific manner. Our group [26] reported a facile preparation of microporous carbons with high specific surface areas (2000−3100 $m^2 \cdot g^{-1}$), large micropore volumes, and narrow pore size distribution using low-cost sawdust as templates.

2.1.2. Soft-template process

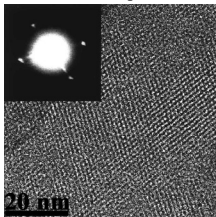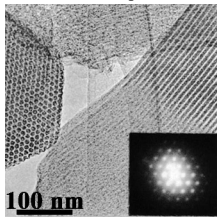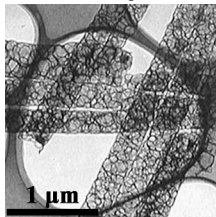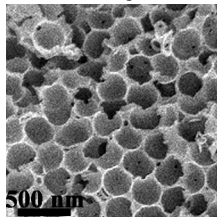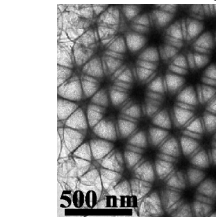Recently, developments in the soft-template synthesis of porous carbon materials have overcome many limitations of hard templates. To reduce the preparation steps, a one-pot approach for achieving the formation of soft-templates coated the carbon precursor shows a good prospect [27,28]. Our group synthesized honeycomb-like hierarchically porous carbons by using tetraethyl orthosilicate (TEOS) as template precursor and phenolic resin as carbon source [29]. This method is more facile and time-saving in comparison with the conventional hard-template methods.

Ordered mesoporous/macroporous carbons have been synthesized with the block copolymers (BCPs) as templates. The selection of a pair of suitable copolymers and surfactant is the most important factor to control the structure of porous carbon. Tanaka et al. [30] used an organic-organic nanocomposite as precursor to fabricate mesoporous carbons (COU-1) with ordered channel structure. At 400 °C, the resorcinol/formaldehyde (RF) polymer remained as pore walls, while the surfactant F127 decomposed to mesopores. The combination of hard and soft templates has also been attempted. Hierarchically porous carbons were fabricated via a solvent evaporation using the lab-prepared silica colloidal crystals as a hard template and the triblock copolymer (Pluronic F127) as a soft template [31].

Table 1 summarizes selected porous carbon materials prepared by template method. Since the hard-template process was proven to synthesize porous carbon in 1980, the technique has been widely developed owing to its fidelity in replicating the structures of templates. However, there is almost no chemical interaction between hard templates and carbon precursors during the replication process. Furthermore, the hard template needs to be removed in the synthesis process, and the stabilities of replicated meso-structures have much room for improvement. On comparison, soft-template method depends on the chemical interactions between templates and carbon precursors such as the hydrogen bond and Coulombic force. It is noted that most porous carbon materials with uniform pore size and high surface area were synthesized by template method since the porous structures can be controlled by the designation of the nanostructure templates. For future research, new synthetic routes such as pairs of soft-templates and carbon precursors and their interactions need to be explored.

Table 1. Synthetic method and morphology of several porous carbon materials prepared by template process

	Ordered microporous carbons	Ordered mesoporous carbons (CMK-3)	CNTs	Hierarchically porous carbons	Ordered macro-/mesoporous carbons
Carbon source	poly(furfuryl alcohol)	sucrose	poly(furfuryl alcohol)	phenolic resin	phenolic resin
Template	zeolite	SBA-15	AAO	silica template	Pluronic F127, silica colloidal crystal
Method	hard-template	hard-template	hard-template	soft-template	hard- & soft-template
Morphology					
Reference	[17]	[18]	[23]	[29]	[31]

2.2. Activation process

Activated carbons are disordered microporous carbons with specific surface area in the range of $800-1500$ $m^2 \cdot g^{-1}$. They are usually produced by CO_2 physical activation and $ZnCl_2$ chemical activation [6,32,33]. Huang's group [34] reported a facile strategy to synthesize nitrogen-doping porous carbon nanofiber webs by carbonization-activation of polypyrrole (PPy) with KOH. Ruoff's group [35] used a simple activation of microwave exfoliated graphite oxide (MEGO) to obtain porous graphene with high specific surface area of 3100 $m^2 \cdot g^{-1}$. Activation process is facile and easy to achieve scalability, but the as-prepared porous carbon materials usually show non-uniform pore sizes and isolated non-interconnected pores.

Table 2 summarizes the textual parameters of typical porous carbon materials. For the electrodes of electrochemical devices, porous carbon materials need high electronic con-ductivity, but many porous carbon materials (e.g., CMK-3) prepared by template method do not show highly graphitic structures that generally influence their electronic conductivity. Commercial conductive carbon black such as Vulcan XC-72 exhibits highly electronic conductivity (2.78 $S \cdot cm^{-1}$), so they have been frequently used in the field of electrochemical storage and conversion. 1D porous carbon materials such as CNTs achieve fast electronic transmission in the 1D direction. Further improvement of the surface area and pore volume of conductive carbon black and CNTs would enhance the infiltrating of electrolytes to obtain better electrochemical properties. Porous graphene has highly electronic conductivity and surface area, while its synthetic process is complicated and high cost. Our group recently reported porous hollow carbon spheres prepared via a facile self-assembly method, which showed a broader pore size distribution (from micropores to mesopores) with large pore volume and a high degree of graphitization [36]. Thus, facile and economical synthetic routes should be developed for the wide application.

Table 2. Textual parameters of typical porous carbon materials

Typical porous carbon	Pore size distribution	Pore volume $(cm^3 \cdot g^{-1})$	BET specific surface area $(m^2 \cdot g^{-1})$	Electronic conductivity $(S \cdot cm^{-1})$	Cost	Synthetic method	References
Vulcan XC-72	mesopores (30 nm)	1.78	254	2.78	low	manufactured by cabot inc.	[37]
CMK-3	mesopores (3.3 nm)	2.1	1976	0.20	high	hard-template method (SBA-15)	[38]
CNT	mesopores (9.9 nm)	0.85	596	0.89	high	hard-template method (AAO)	[39]
Porous graphene	mesopores and micropores	2.14	3100	$\sim$5	high	chemical activation	[35]
Hierarchically porous carbons	mesopores and micropores	2.61	1520	2.22	moderate	soft-template method	[36]

3. Applications of functional porous carbon-based composite electrode materials

In modern society, people have widely used reliable devices which depend on electrochemical energy storage and conversion such as batteries and fuel cells. Most electrode materials are the composites of conductive carbons, binding agent, and inorganic compounds. Porous carbon materials have excellent properties and are easily incorporated with inorganic compounds by melt-diffusion strategy [38], wet impregnation [40], grinding process [41], ball milling [42], sonochemical method [43], and sol-gel process [44]. In the following contents, we mainly introduce the recent developments of the composite electrode materials of porous carbons and inorganic compounds in the field of LIBs, Li-S batteries, and Li-O_2 batteries.

3.1. Lithium-ion batteries

During the past three decades, a wide variety of electrode materials have been investigated for LIBs [45−48]. The cathode materials have focused on layered lithiated transition metal oxides (e.g., LiNi$_{1/3}$Mn$_{1/3}$Co$_{1/3}$O$_2$), spinel-type compounds (e.g., LiMn$_2$O$_4$ and LiNi$_{0.5}$Mn$_{1.5}$O$_4$), polyanion-based compounds (e.g., LiFePO$_4$ and Li$_2$FeSiO$_4$); While the anode materials are concentrated on C, Si, Sn or their alloys/compounds, and transition metal oxides (e.g., Fe$_3$O$_4$, Mn$_3$O$_4$ and Li$_4$Ti$_5$O$_{12}$). However, LIBs have suffered the following problems. First, some semiconductor or insulator electrode materials (e.g., Li$_4$Ti$_5$O$_{12}$, Si, LiFePO$_4$, and Li$_2$FeSiO$_4$) suffer sluggish electrochemical kinetics. Second, some compounds (e.g., Si, Fe$_3$O$_4$, and SnO$_2$) have large structural or volume change, leading to poor cycling performance. Third, nanoparticles grow and agglomerate during the preparation process [49]. In order to overcome these disadvantages, porous carbon serves as a conductive matrix to be incorporated with the active materials. Porous carbons have higher electronic conductivity ($0.1-3$ $S \cdot cm^{-1}$) than that of semiconducting and insulating electrodes ($10^{-9}-10^{-14}$ $S \cdot cm^{-1}$). Meanwhile, porous carbons increase the electrode-electrolyte interfacial area and provide efficient ion transport paths to improve Li$^+$ ion transport kinetics. As shown in Figure 2, electrons can fast transport in the pore walls and Li$^+$ ions can fast diffuse along the channels.

3.1.1. Anode

Anode materials for LIBs mainly include carbon materials, transition metal oxides, Si or Sn-based materials, and
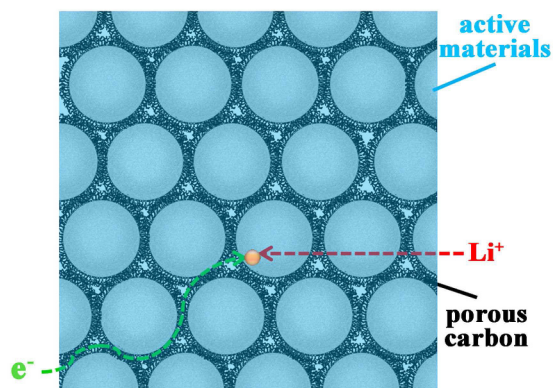
Figure 2. Schematic illustration of e$^-$ and Li$^+$ transports in the composite electrode materials of porous carbons and inorganic compounds

spinel-type Li$_4$Ti$_5$O$_{12}$. In the case of porous carbon, lithium ions first insert into graphite crystallites, and later enter into micropores [50]. The number of micropores and the reversible capacity are direct proportion. Mesopores provide the channels of Li$^+$ ion transport and enhance the infiltration of electrolyte. Therefore, porous carbons have been considered as improving anode materials because they show higher capacities (400−700 mAh·g^{-1}) than those of graphite (372 mAh·g^{-1}). However, large irreversible capacity of porous carbons during the first cycle limits their developments. To further enhance the electrochemical performance of porous carbon anode, loading transition metal oxides is a feasible strategy. Zhang et al. [51] reported a CoO/CMK-3 nanocomposite by an impregnating method using Co(NO$_3$)$_2$·6H$_2$O as the cobalt source, which showed better specific capacity, coulombic efficiency, and cycling performance compared with those of CMK-3. CoO nanoparticles were loaded to reduce the surface area of the CMK-3, so the formation of the solid electrolyte interface (SEI) films was restrained.

In the case of transition metal oxides (e.g., Fe$_2$O$_3$, Co$_3$O$_4$, and NiO), it is suggested that active materials take place a "conversion reaction" that transition metal oxides react with lithium ions to form metal substance and Li$_2$O [52−54]. In this process, the crystal structure of transition metal oxide changes tremendously during cycling, leading to remarkable volume variations and severe aggregation. For solving this problem, transition metal oxides are embedded in porous carbon matrix. Lee's group [55] successfully synthesized the composite of Fe$_3$O$_4$ nanocrystals impregnated mesoporous carbon foams (CFs) using Fe(NO$_3$)$_3$ as raw material. The composite showed more than 780 mAh·g^{-1} after 50 cycles. The CFs widely dispersed Fe$_3$O$_4$ nanocrystals to prevent their agglomeration, reducing the capacity fade during charge/discharge processes. A graphitic mesoporous carbon/MoO$_2$ nanocomposite was also prepared by an impregnation method [56]. The graphitic carbon matrix constrained the growth of MoO$_2$ particles and enhanced Li$^+$ ion and electron transport. The nanocomposite showed a high reversible capacity of 760 mAh·g^{-1}. Garcia and co-workers [57] developed a facile method for simultaneous formation of

Fe$_3$O$_4$ nanoparticles and porous carbon by heating Fe alginate aerogel with a high surface area and porosity. This method uses biomass waste as raw materials and does not need presynthesis of porous carbon. In addition, the as-prepared composite showed a reversible capacity of 702 mAh·g^{-1} after 50 cycles.

Manganese oxides (e.g., MnO$_2$, Mn$_3$O$_4$, and MnO) are attractive inorganic materials because of their wide applications in batteries. Li et al. [58] developed an impregnating route to prepare Mn$_3$O$_4$ nanoparticles embedded within ordered mesoporous carbon (CMK-3) for LIBs. The Mn$_3$O$_4$/CMK-3 composite displayed a specific capacity of 802 mAh·g^{-1}, and a high coulombic efficiency of up to 99.2% after 50 cycles at a high current density of 100 mA·g^{-1}. The enhanced electrochemical performance of the Mn$_3$O$_4$/CMK-3 composite was attributed to its ordered mesoporous structure, which buffered well against the local volume change during the charge-discharge processes, shortened the transport length for Li$^+$ ion diffusion, and improved the electrolyte infiltration. Besides Mn$_3$O$_4$, MnO was also impregnated into the porous carbon by a microwave-polyol process without templates [59]. The as-prepared porous carbon/MnO disk composite exhibited an average thickness of 50 nm and diameters of about 3 mm with a large specific surface area of 75.3 m^2·g^{-1}. The composite showed a discharge capacity of 534.6 mAh·g^{-1} after 250 cycles at a high current density of 1000 mA·g^{-1}.

Si and Sn-based materials are considered to be promising anode because of their high theoretical specific capacity. Si has ultrahigh theoretical specific capacity (4200 mAh·g^{-1}), which is about 11 times higher than that of the current commercial graphite anode [60]. However, Si undergoes a huge volume expansion (up to 300%) during charge and discharge processes, leading to poor cycling stability [61]. Porous carbons have large pore volume which constrains the volume swings. Jeong et al. [62] prepared Si nanoparticles embedded in porous nitrogen-doped carbon spheres (NCSs). The porous structure of NCSs buffered the volume expansion of Si nanoparticles and improved contacts between Si and carbon conductors. The composite electrode exhibits a high capacity of 1579 mAh·g^{-1} at 0.1C rate based on the mass of both Si and C, and the capacity kept 94% after 300 cycles. Tin-based oxides have also drawn a lot of attention due to their high theoretical specific capacity. However, the volume change of up to 200% limits their development. Zhao's group reported that the composite of SnO$_2$ and ordered mesoporous carbon synthesized via a full-deposition method showed stable cycling performance [63].

Lithium titanate (Li$_4$Ti$_5$O$_{12}$) with spinel structure has recently attracted intention as a promising anode due to high rate performance, cyclic stability, flat operation potential plateau, and reliable security [64,65]. Furthermore, the spinel Li$_4$Ti$_5$O$_{12}$ is a zero-strain insertion material with no volume change during cycling. However, spinel Li$_4$Ti$_5$O$_{12}$ suffers from low electrical conductivity (<10^{-13} S·cm^{-1}), leading to sluggish electrochemical kinetics. In order to overcome this disadvantage and improve the performance of Li$_4$Ti$_5$O$_{12}$, porous carbons serve as a conductive matrix to encapsulate

$Li_4Ti_5O_{12}$. Shen et al. [66] designed a nanocasting method to synthesize $Li_4Ti_5O_{12}$/CMK-3 composite, in which the ordered mesoporous CMK-3 is used as the stable nanostructured matrix and $Li_4Ti_5O_{12}$ is the active material. The CMK-3 not only serves as a conductive matrix that provides a quick electron transport, but also acts as a reaction vessel for the $Li_4Ti_5O_{12}$ precursor, which prevents agglomeration of the

$Li_4Ti_5O_{12}$ particles during the heat treatment. Furthermore, various nanochannels provide a large contact area between the electrolyte and the electrode, ensuring that the electrolyte can easily infuse the mesopores. As shown in Figure 3, the $Li_4Ti_5O_{12}$/CMK-3 nanocomposite shows a high capacity of $92.6\ mAh \cdot g^{-1}$ at 40C and only 5.6% capacity loss after 1000 cycles at 20C.
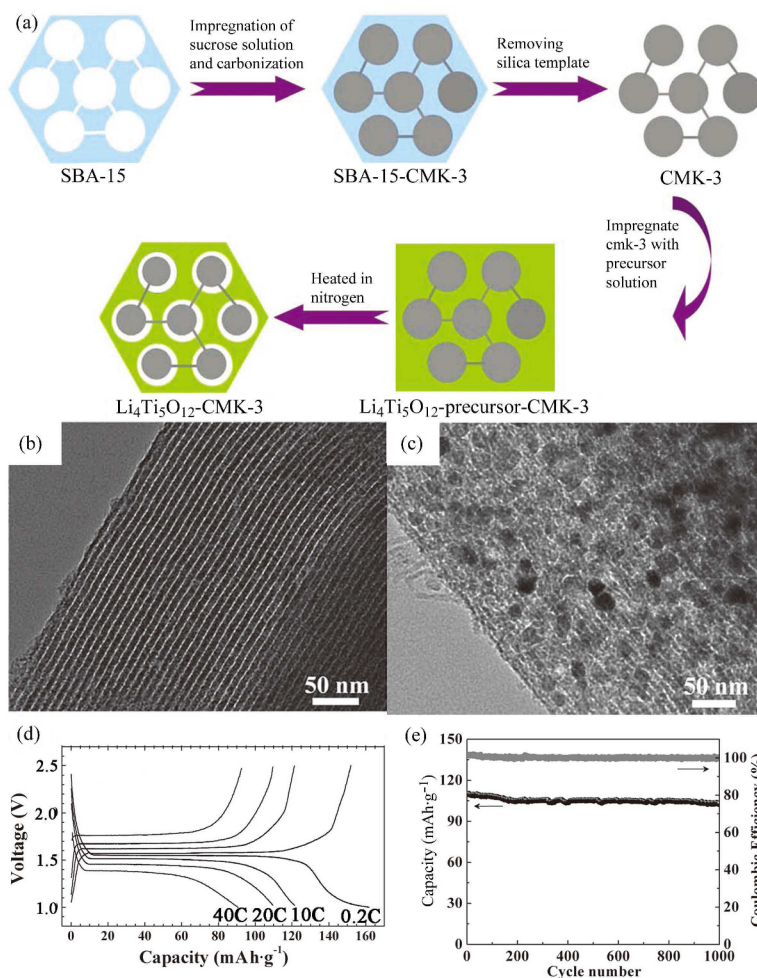

Figure 3. (a) Schematic illustration of the synthesis of mesoporous $Li_4Ti_5O_{12}$/CMK-3 nanocomposite, (b) TEM images of a CMK-3 carbon template, (c) TEM images of mesoporous $Li_4Ti_5O_{12}$/CMK-3 nanocomposite, (d) galvanostatic charge-discharge curves of mesoporous $Li_4Ti_5O_{12}$/CMK-3 nanocomposite electrode at different rates, and (e) specific capacity and coulombic efficiency of mesoporous $Li_4Ti_5O_{12}$/CMK-3 nanocomposite for 1000 cycles at a rate of 20 C [66]. Copyright 2012, Wiley-VCH.

3.1.2. Cathode

Up to now, three types of materials including layered lithiated transition metal oxides, Mn-based spinels and polyanion-type compounds have been studied as the cathode of LIBs [47]. Among them, polyanion compounds are promising candidate for cathode materials because they show facile synthetic routes, high specific capacity, low cost, environmentally friendly, and high thermal stability. $LiFePO_4$, which was firstly studied by Goodenough [67], has been widely investigated in the last decade. However, olivine structure $LiFePO_4$ suffers from low intrinsic elec-

tric conductivity ($\sim 10^{-9}\ S \cdot cm^{-1}$) and sluggish one dimension Li^+ ion transport [68]. Porous carbons can improve the ionic- and electronic-transport limitations, and thus they have been widely used for improving the electronic conductivities of electrode materials. Wu et al. [44] proposed a new nanostructure design of electrode materials for high-power and high-energy lithium batteries by combining the advantages of nanoporous carbon and nanometer-sized active particles. The nanocomposite of $LiFePO_4$ nanoparticles embedded in nanoporous carbon matrix (defined as NP@NPCM) was synthesized by a facile method combining both a sol-gel procedure and a solid-state reaction using a

block copolymer (Pluronic F127) as a nanopore-forming soft-template. LiFePO$_4$ nanoparticles were highly dispersed into the nanoporous carbon matrix and their particle sizes were small, which significantly shorten the diffusion time of Li$^+$ ions in the crystal lattice. Furthermore, nanoporous carbon matrix with various pores served not only as a conducting 3D network for providing path of both Li$^+$ ions and electrons transport, but also as an vessel to enhance the infiltration of electrolyte. The LFP-NP@NPCM nanocomposite showed a high discharge energy density of 87 Wh·kg^{-1} at a high power density of 20 kW·kg^{-1} (230C). The discharge capacity only decayed ∼3% after 700 cycles at 1.5C rate. Similarly, Li$_2$FeSiO$_4$ also draws a great promise as a potential cathode material because of its high specific theoretical capacity (330 mAh·g^{-1} if the second Li$^+$ exchange could be achieved). Furthermore, Li$_2$FeSiO$_4$ is low cost, high safety, and nontoxicity. However, Li$_2$FeSiO$_4$ exhibits low electronic conductivity (6×10^{-14} S·cm^{-1}) and ion transmittability [69], which limits its electrochemical capacity, cycling stability, and rate performance. Recent studies show that coating conductive porous carbons has proven to be an efficient strategy in enhancing the electrochemical performance of Li$_2$FeSiO$_4$. Zheng et al. [12] reported on the synthesis of porous Li$_2$FeSiO$_4$/C nanocomposites via a tartaric acid (TA) assisted sol-gel method (Figure 4). Li$_2$FeSiO$_4$/C nanocomposites with the size around 30 nm exhibited high electronic conductivity (1.63×10^{-3} S·cm^{-1}) and Li$^+$ diffusion coefficient (1.46×10^{-12} cm^2·s^{-1}), showing the initial discharge capacity of 155.3 mAh·g^{-1} and a reversible capacity of 132.1 mAh·g^{-1} after 50 cycles at 1C rate.
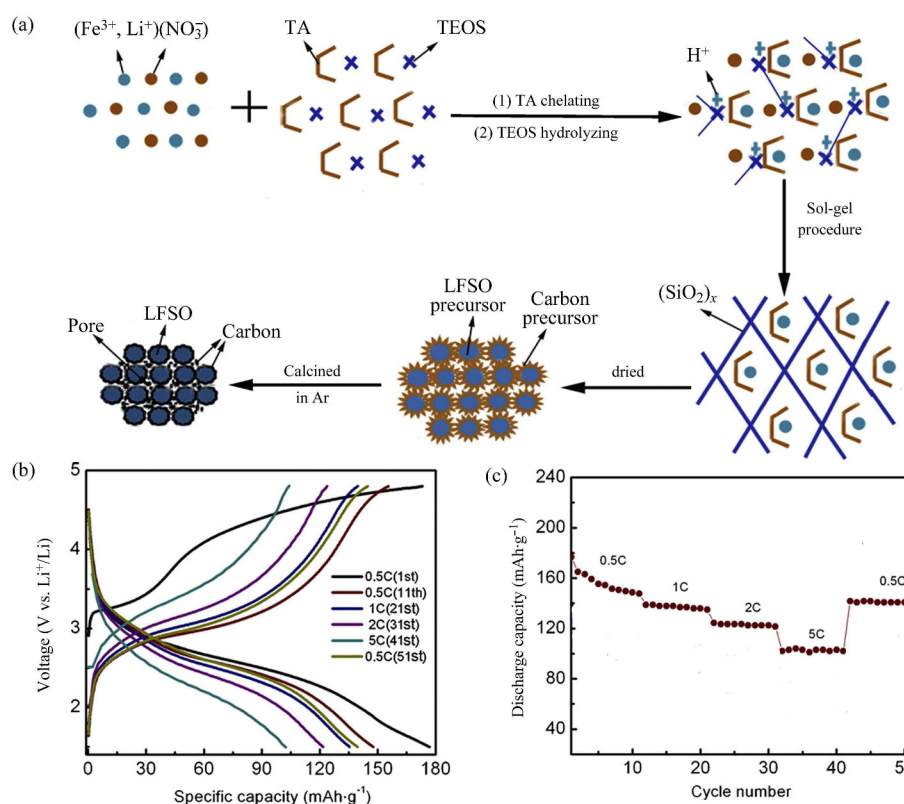

Figure 4. (a) Schematic illustration of the preparation of porous Li$_2$FeSiO$_4$/C nanocomposite, (b) charge-discharge curves of porous Li$_2$FeSiO$_4$/C nanocomposite, and (c) its corresponding capacity performance continuously cycled at 0.5, 1, 2, 5, and 0.5 C [12]. Copyright 2012, Elsevier

Some organic molecules can also be impregnated into the porous carbon [70], but they are easily sublimated. The improvement of electrochemical performance is slight, making them less significant than inorganic compounds. Therefore, the composite electrode materials of porous carbons and inorganic compounds are more important for LIBs. The synthetic methods of the composite electrode materials of porous carbons and inorganic compounds can be divided into two categories: impregnation method and in situ synthesis. Impregnation of the precursors or solvents containing the active materials makes the surface areas of pristine porous carbons decrease, but their surface areas are still higher than those of the composite electrode materials prepared by in situ synthesis such as sol-gel method. As listed in Table 3, the two methods can prepare the composite electrode materials with both high degree of graphitization and electrochemical performance. For impregnation method, active materials should be entirely impregnated in the pores with high load; While for in situ synthesis, improving the surface area and preparing the ordered porous structure should be explored.

Table 3. Textual parameters of several composite electrodes

Composite electrode	I_D/I_G	BET specific surface area ($m^2 \cdot g^{-1}$)	Discharge capacity ($mAh \cdot g^{-1}$)	Synthetic method	References
Mn_3O_4@C	–	708	802 (100 $mA \cdot g^{-1}$)	impregnation	[58]
$Li_4Ti_5O_{12}$@C	∼1	127	161.7 (0.2C), 73.4 (80C)	impregnation	[66]
Si@C	–	244	1571 (0.1C), 702 (10C)	impregnation	[71]
$LiFePO_4$@C	∼0.8	101.3	∼145 (C/9), ∼40 (230C)	sol-gel method	[44]
Li_2FeSiO_4@C	0.99	64.4	176.8 (0.5C)	sol-gel method	[12]

The advantages of porous carbons in the field of LIBs are summarized in the following aspects. (1) The porous structure is good for the liquid electrolyte to infiltrate into the electrode materials and provides fast conductive transport channels for the Li$^+$ ions. The channels of the porous carbons also constrain the local volume change during the charge and discharge processes and enhance the structural stability. (2) The improved performance can be attributed to good electrical contact between nanoparticles and porous carbons. The porous carbons are well conductive network between nanoparticles, which reduce the inner resistance of the LIBs and enhance the electronic and ionic conductivity, leading to higher performance. (3) The porous carbons are also reaction vessels to prepare nanoparticles. As known, Li$^+$ ion diffusion strongly depends on the transport length and active sites on the surface of the active materials. Porous carbons increase the contact area between the electrode and the electrolyte, shortening the path length for Li$^+$ ion transport, and offering improved electrochemical performance. (4) The porous carbons efficiently prevent the aggregation and growth of nanoparticles and the cracking of the electrode materials during continuous cycles. Thus, high capacity, high coulombic efficiency, high rate capability and stable cycling performance are obtained. Based on the above analysis, porous carbons are ideal matrixes to composite inorganic compounds for LIBs.

3.2. Li-S batteries

Li-S batteries recently have attracted increasing attention because of their high specific capacity (1675 $mAh \cdot g^{-1}$) and energy density (2600 $Wh \cdot kg^{-1}$). Furthermore, sulfur is abundant, low-cost, and environmental friendliness [72−76]. However, Li-S batteries encounter the following difficulties. First, sulfur is electrically insulating, leading to a poor electronic conductivity (5×10^{-30} $S \cdot cm^{-1}$) and rate capability. Second, the electrochemical reactions are associated with a series of electron and phase transitions. The intermediate long chain polysulfides are severely soluble in conventional organic electrolytes. The dissolved polysulfides migrate to the Li anode, and then react with Li to form shorter chain polysulfides. These reactions consequently result in the severe anode corrosion and the rapid increase of the internal resistance. This "shuttle" phenomenon causes poor cycle ability and low coulombic efficiency. Third, volume expansion of sulfur is large during the charge-discharge processes, so the capacity fades seriously. Porous carbons with high electronic conductivity, strong adsorption capacity, and good porous structure can solve the above problems [77]. Thus, various porous carbon-sulfur composites have been prepared to obtain high performance of Li-S batteries.

Nazar's group [38] prepared a polyethylene glycol (PEG) modified CMK-3/S nanocomposite with 70 wt% sulfur which showed an initial discharge capacity of 1320 $mAh \cdot g^{-1}$ and a reversible capacity of 1100 $mAh \cdot g^{-1}$ after 20 cycles. The CMK-3 repressed sulfur growth within its channels and improved essential electrical contact with the insulating sulfur. The mesoporous structure provided path to Li$^+$ ions transport and enhanced the diffusion kinetic of Li$^+$ ions and electron. Polymer modification of the carbon surface further provided a chemical gradient that constrained diffusion of the polysufides out of the electrode.

The relationship between the pore size and pore volume of mesoporous carbon and the performance of its composite electrode was also systematically investigated [78]. The results revealed that mesoporous carbon with a larger pore volume can load more sulfur, but overall the electrochemical performance is very similar for different composites at full sulfur-filling conditions. For the same mesoporous carbon, partial sulfur-filling improved the initial discharge capacity and cycle stability due to improved electrical and ionic transport during charge-discharge processes. Therefore, a large pore volume, partial sulfur filling, and polymer coating were a good designation for Li-S batteries. The poly(3, 4-ethylenedioxythiophene)poly(styrenesulfonate) (PEDT/PSS)-coating carbon-sulfur with 50 wt% sulfur showed an initial capacity of 1390 $mAh \cdot g^{-1}$ and a capacity retention of 840 $mAh \cdot g^{-1}$ over 100 cycles at 0.1C rate.

The combination of mesopores and micropores is a good way to improve the performance of Li-S batteries. Liang and co-aurthors [79] activated the mesoporous carbon prepared by a soft-template to obtain a carbon material with two types of pores. This porous carbon material with mesopores (7.3 nm) and micropores (<2 nm) is a suitable matrix for the carbon-sulfur composite. The high surface area was mainly from micropores which retain the sublimed sulfur and the mesoporoes which provide a path for the mass transport of Li$^+$ ions.

Microporous carbon-sulfur composite has also potential application for Li-S batteries due to its electrochemical cycle stability. Aurbach and co-workers reported [80] a novel composite, in which sublimed sulfur was impregnated microporous activated carbon fibers (ACF) to form monolithic electrodes. The ACF-S composite cathode, which was binder free, showed a reversible discharge capacity of more than 800 $mAh \cdot g^{-1}$ after 80 cycles. The microporous structure enhanced electrolyte infiltration and decreased the solution of

the polysulfides.

Porous hollow carbon spheres with large pore volume are proved to be effective host to maximize the polysulfides dissolution in the organic electrolyte and improve the electronic conductivity of the electrode [81]. Our group [36] reported the promising electrochemical performance of the carbon-sulfur composite, in which sulfur was impregnated into the porous hollow carbon spheres (PHCSs) via a melt-diffusion method. The PHCSs showed the characteristics of high specific surface area (1520 m^2·g^{-1}), large pore volume (2.61 cm^3·g^{-1}), broad pore size distribution from micropores to mesopores, and high electronic conductivity (2.22 S·cm^{-1}). As shown in Figure 5, the carbon-sulfur composite displays an initial discharge capacity of 1450 mAh·g^{-1} (which is 86.6% of the theoretical specific capacity) and a reversible discharge capacity of 1357 mAh·g^{-1} after 50 cycles at 0.05C charge-discharge rate. At higher rate of 0.5C, the capacity is stabilized at around 800 mAh·g^{-1} after 50 cycles.
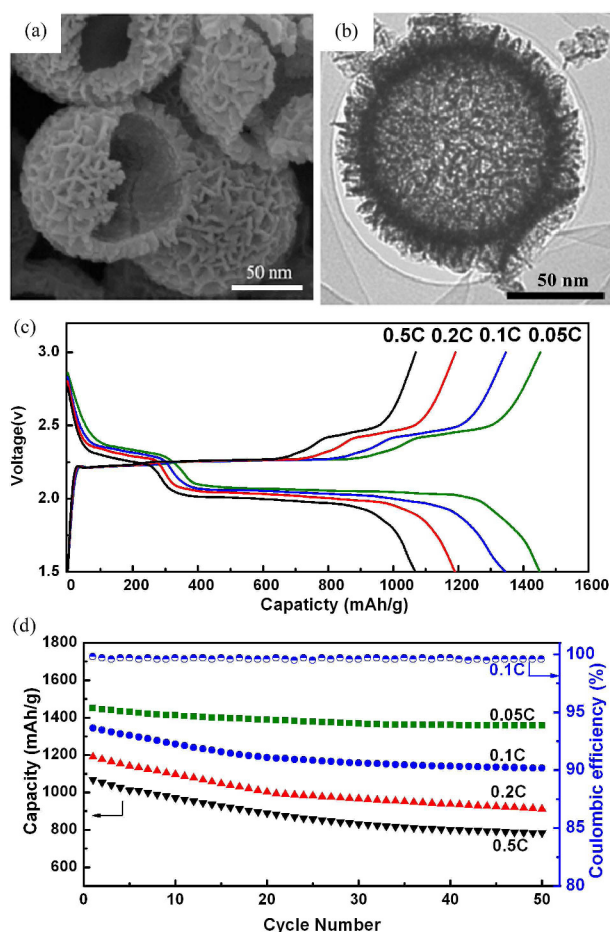

Figure 5. SEM (a), TEM (b), discharge and charge curves (c), and cycling performance (d) of carbon-sulfur composite [36]. Copyright 2013, Springer-Link

Improving electrochemical performance of Li-S batteries with porous carbon can be understood from the following aspect. First, the porous structure is advantageous for sulfur adsorption, so sulfur exists as high dispersed state. Second, the porous structure immensely reduces the dissolution of polysulfides, which minimizes the shuttling loss. It is suggested that mesopores enable carbon-sulfur composites to have a high initial discharge capacity, and micropores improve the cycle life. Third, high pore volume provides large space to accommodate the volume expansion of the sulfur, preventing the structure change of the cathode. Last, porous carbons are superior electronic conductivity, improving the electron transport of the carbon-sulfur composite cathode. Therefore, the porous carbon-sulfur composites can be used as potential cathode materials of Li-S batteries.

As similar as S, elemental phosphorus is another potentially attractive material with a theoretical specific capacity of 2595 mAh·g^{-1} [82]. Phosphorus has three main allotropes (i.e., white, red, and black). White phosphorus is poor chemical stability and black phosphorus is the most difficult to be prepared, so red phosphorus is a suitable electrode material. However, it is also an electronic insulator and its experimental capacity is very low and dramatically fades during cycles. He's group [42] demonstrated a vaporization/adsorption strategy to prepare a nanostructured composite of red phosphorus and porous carbon. The composite showed a high reversible capacity of more than 750 mAh·g^{-1} based on the porous carbon-phosphorus composite and 2413 mAh·g^{-1} based on red phosphorus. The results showed that porous carbon enhances the electrochemical performance of red phosphorus.

3.3. Li-O$_2$ batteries

Li-O$_2$ batteries are composed by a Li anode and an air electrode with open structure to absorb oxygen. Electrocatalysts for the ORR have also been one of the main focuses of electrochemistry in the field of Li-O$_2$ batteries. Oxygen reduction can proceed via two pathways (Figure 6): One is a two-electron (2e) pathway that forms hydrogen peroxide species as intermediates, and another is a four-electron (4e) process to produce water or hydroxides as the end product [83,84]. The ORR pathways connect with the O$_2$ adsorption configurations and the O$_2$-surface interactions. ORR catalysts include Pt/Pt-base and non-Pt materials. Pt/Pt-base alloys have been the most widely studied. The porous carbons are favorable to increase the density and utilization of active sites and optimize the catalyst synthesis strategies and conditions for achieving better activity and stability. The porous carbons make ORR catalysts highly dispersed to promise the electrocatalytic activity for oxygen reduction, and the porous structure provides space of gas diffusion and interface area of three phase reaction. Recently, various porous carbons have been used as the catalyst support to synthesize highly dispersed nanoparticles.

Inorganic nanoparticles are usually dispersed on the carbon materials with high surface area, electronic conductivity, and electrochemical stability to make ORR electrocatalysts. Vulcan XC-72 is the most conventional catalyst support in literatures. Moreover, CNTs and other porous carbon (e.g.,

CMK-3) have also attracted increasing interests [39,41,85]. Neat Vulcan XC-72 obviously contributes to the ORR kinetics, but it shows high overpotential and low activity. In addition, Vulcan XC-72 has large micropore volume, leading to inferior utilization of catalysts. CNTs match the requirements of catalyst support and can also serve as electrode materials [86,87].
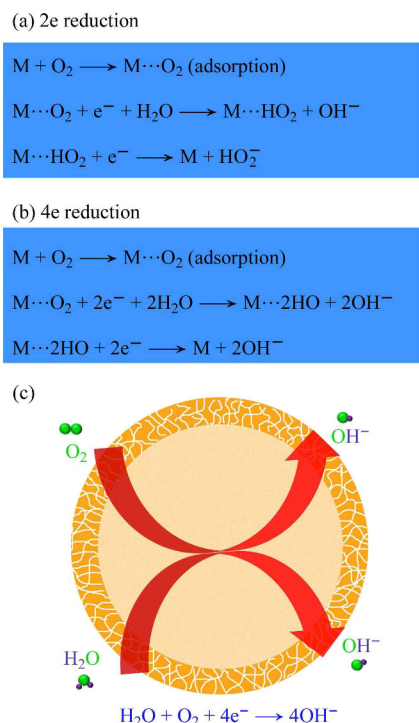

Figure 6. Simplified electrochemical catalysis process of the ORR. (a) 2e reduction, (b) and (c) 4e reduction

Recently, ordered mesoporous carbon such as CMK-3 has been used as an ideal matrix for hosting the precursors to prepare highly dispersed nanoparticles. Joo et al. [88] synthesized highly dispersed platinum nanoparticles in nanoporous carbons, and the platinum cluster diameter is below 3 nm. The Pt/nanoporous carbon shows a surprisingly high peak activity amounting to 100 $A \cdot g^{-1}$ at the 33 wt% Pt loading, which proves to promise electrocatalytic activity for ORR. Xia's group [89] prepared Mn_3O_4 nanoparticles with 10 nm size which were attached to the outer surface of CMK-3, rather than being embedded in the pores of CMK-3. The electrocatalytic performance for ORR of the Mn_3O_4/CMK-3 composite was better than that of the other carbon-based composite catalysts (carbon nanotubes, activated carbon, and graphite). Since the ordered mesopores of CMK-3 provide available gas diffusion channels, the Mn_3O_4/CMK-3 composite provides enough effective three-phase interface area, which is very important for the complex three-phase interface electrocatalytic reaction.

The oxygen evolution reactions (OER) also play a key role in rechargeable metal-air batteries. Porous carbon materials (e.g., Vulcan XC-72) can also serve as catalyst support material and catalyze the OER, but it is featured with

low activity [90]. As similar as ORR, porous carbon materials make catalysts highly dispersed to acquire high activity and durability.

Among various metal-air batteries, Li-O_2 batteries have the highest theoretical special energy density (11400 $Wh \cdot kg^{-1}$). During the discharge process, oxygen is reduced on an air electrode to form peroxide ion and then reacts with Li^+ ions to produce Li_2O_2. The functional porous carbon-based composite electrode materials have been used as air electrode because the pores as reactors facilitate the diffusion of oxygen and inhibit the aggregation of Li_2O_2. Zhang's group [91] synthesized graphene oxide gel-derived, binder-free, hierarchically porous carbons in nickel foam by in situ sol-gel method. The discharge capacity reached 11060 $mAh \cdot g^{-1}$ at a current density of 0.28 $A \cdot g^{-1}$ and 2020 $mAh \cdot g^{-1}$ at a high current density of 2.8 $A \cdot g^{-1}$. Wang and co-authors [40] reported a nanocomposite of CoO and CMK-3 as an air electrode for Li-O_2 batteries. The mesopores of CMK-3 were propitious to the diffusion of oxygen and the release of subsidiary products. The CoO nanoparticles significantly reduced the charge platform and improved the cycle performance.

For Li-O_2 batteries, during the synthetic process, the pores strain the agglomeration of particles, and highly dispersed nanoparticles are obtained. This method can not only produce nanoscale materials, but also support small metal or metal oxide particles for electrocatalytic applications. On one hand, highly dispersed nanoparticles have large specific surface areas, which save the amount of metals and metal oxides. On the other hand, the particle size with selected crystalline face can change the catalytic selectivity to achieve high performance. Mesoporous carbons with thicker crystalline walls and larger pore size are suitable to serve as catalyst support materials, and ordered mesoporous carbon facilitates three-phase interface electrocatalytic reaction.

4. Summary and outlook

In summary, recent advances in the functional porous carbon-based composites as electrode materials have been reviewed. In particular, porous carbons with the incorporation of metals (Pt), non-metals (Si, S, and P), metal oxides (SnO_2, MnO_2, and Fe_3O_4), spinel-type compounds ($Li_4Ti_5O_{12}$) and polyanion-type compounds ($LiFePO_4$ and Li_2FeSiO_4) as the composite materials show excellent electrochemical performance.

The design and synthesis of porous carbon are the basis of preparation of composite electrode. Many synthetic methods have been proposed to obtain porous carbons with various pore distribution, pore volume, surface area, wall thickness, and electronic conductivity. Among them, template process has proven to be the most successful routes for the fabrication of porous carbon with well-defined pore structures and narrow pore-size distributions. The porous channels are also used as nano-reactors to prepare nanoparticles. Intensive study in this area would focus on the design of porous carbons with high densities.

Lithium secondary batteries have been widely used for energy conversion and storage because of their high energy density. For LIBs, the porous structure of electrode is in favor of the electrolyte infiltration. Micropores can store Li^+ ions, mesopores can provide fast transport channels for Li^+ ions, and macropores can accommodate the volume change during the charge and discharge processes. Furthermore, the porous carbons efficiently prevent the nanoparticles from aggregation and furnish a 3D conductive network between nanoparticles. Large pore volume is favorable to enhance the load of active materials. A combination of high specific capacity, high coulombic efficiency, high rate capability and stable cycling performance of the electrode with composite materials is achieved by using the porous carbon based composites. As to Li-S batteries, the porous structure makes sulfur exist as highly dispersed state. The porous carbon materials provide large space to resist the volume expansion of the sulfur and improve the electron transport of the carbon-sulfur composite cathode. Mesopores can enhance the initial discharge capacity of carbon-sulfur composites and micropores can effectively restrain the shuttling loss to improve the cycle life. Therefore, the porous carbon-sulfur composites show the potential of Li-S batteries with ultrahigh performance. In the field of $Li-O_2$ batteries, the channels of porous carbons play a role of individual nanoscale reactor with highly dispersed nanoparticles to obtain high electrocatalytic performance. Mesoporous carbon with large surface area, high electronic conductivity, and large chemical stability is proper to serve as catalyst support materials, and ordered mesoporous carbon facilitates three-phase interface electrocatalytic reaction. During the discharge process, the porous structure facilitates the diffusion of oxygen and inhibits the aggregation of Li_2O_2. During the charge process, the pores supply the room to release the subsidiary products.

Porous carbons are ideal matrixes to be incorporated with inorganic compounds for lithium secondary batteries. However, the challenges for further development of composite electrode materials of porous carbons and inorganic compounds still exist in three aspects. First, the synthesis of porous carbons is usually complicated by using the hard or soft templates and harsh conditions. Second, the porous structure may be destroyed during the electrochemical reaction process. Third, the graphitization degree to enhance the electric conductivity and the valid material load are the basic standard for deciding whether the porous carbons are worth of studying or commercializing. Therefore, large-scale application of porous carbons in electrochemical devices needs the combination of a facile synthesis route, a stable porous structure, a high graphitization, and a high load of the active materials. Further exploration and development of functional porous carbon-based composite materials should be favorable to meet the ever-increasing requirements for the modern society.

References

[1] Che G, Lakshmi B B, Fisher E R, Martin C R. *Nature*, 1998, 393: 346

[2] Zhu Y, James D K, Tour J M. *Adv Mater*, 2012, 24: 4924

[3] Nishihara H, Kyotani T. *Adv Mater*, 2012, 24: 4473

[4] Zhang L L, Zhao X S. *Chem Soc Rev*, 2009, 38: 2520

[5] Lee J, Kim J, Hyeon T. *Adv Mater*, 2006, 18: 2073

[6] Tamai H, Kakii T, Hirota Y, Kumamoto T, Yasuda H. *Chem Mater*, 1996, 8: 454

[7] Zhou H, Li G, Wang X, Jin C, Chen Y. *J Nat Gas Chem*, 2009, 18: 365

[8] Stein A, Wang Z, Fierke M. *Adv Mater*, 2009, 21: 265

[9] Liang C, Li Z, Dai S. *Angew Chem Int Ed*, 2008, 47: 3696

[10] Rashidi A M, Lotfi R, Nouralishahi A, Khodagholi M A, Zare M, Eslamipour F. *J Nat Gas Chem*, 2011, 20: 664

[11] Hu Y S, Adelhelm P, Smarsly B M, Hore S, Antonietti M, Maier J. *Adv Funct Mater*, 2007, 17: 1873

[12] Zheng Z, Wang Y, Zhang A, Zhang T, Cheng F, Tao Z, Chen J. *J Power Sources*, 2012, 198: 229

[13] Yoo H, Jo M, Jin B S, Kim H S, Cho J. *Adv Energy Mater*, 2011, 1: 347

[14] Ryoo R, Joo S H, Jun S. *J Phys Chem B*, 1999, 103: 7743

[15] Hu Z, Srinivasan M P, Ni Y. *Adv Mater*, 2000, 12: 62

[16] Kyotani T, Nagai T, Inoue S, Tomita A. *Chem Mater*, 1997, 9: 609

[17] Ma Z, Kyotani T, Liu Z, Terasaki O, Tomita A. *Chem Mater*, 2001, 13: 4413

[18] Jun S, Joo S H, Ryoo R, Kruk M, Jaroniec M, Liu Z, Ohsuna T, Terasaki O. *J Am Chem Soc*, 2000, 122: 10712

[19] Kim T W, Park I S, Ryoo, R. *Angew Chem Int Ed*, 2003, 42: 4375

[20] Xia Y, Mokaya R. *Adv Mater*, 2004, 16: 1553

[21] Fuertes A B. *J Mater Chem*, 2003, 13: 3085

[22] Oda Y, Fukuyama K, Nishikawa K, Namba S, Yoshitake H, Tatsumi T. *Chem Mater*, 2004, 16: 3860

[23] Kyotani T, Tsai L F, Tomita A. *Chem Mater*, 1996, 8: 2109

[24] Kyotani T, Tsai L F, Tomita A. *Chem Mater*, 1995, 7: 1427

[25] Zakhidov A A, Baughman R H, Iqbal Z, Cui C, Khayrullin I, Dantas S O, Marti J, Ralchenko V G. *Science*, 1998, 282: 897

[26] Cheng F, Liang J, Zhao J, Tao Z, Chen J. *Chem Mater*, 2008, 20: 1889

[27] Kawashima D, Aihara T, Kobayashi Y, Kyotani T, Tomita A. *Chem Mater*, 2000, 12: 3397

[28] Sun B, Li G, Wang X. *J Nat Gas Chem*, 2010, 19: 471

[29] Zhao J, Cheng F, Yi C, Liang J, Tao Z, Chen J. *J Mater Chem*, 2009, 19: 4108

[30] Tanaka S, Nishiyama N, Egashira Y, Ueyama K. *Chem Commun*, 2005, 2125

[31] Deng Y, Liu C, Yu T, Liu F, Zhang F, Wan Y, Zhang L, Wang C, Tu B, Webley P A, Wang H, Zhao D. *Chem Mater*, 2007, 19: 3271

[32] Hussein M Z, Tarmizi R S H, Zainal Z, Ibrahim R, Badri M. *Carbon*, 1996, 34: 1447

[33] Miyamoto J, Kanoh H, Kaneko K. *Carbon*, 2005, 43: 855

[34] Qie L, Chen W, Wang Z, Shao Q, Li X, Yuan L, Hu X, Zhang W, Huang Y. *Adv Mater*, 2012, 24: 2047

[35] Zhu Y, Murali S, Stoller M D, Ganesh K J, Cai W, Ferreira P J, Pirkle A, Wallace R M, Cychosz K A, Thommes M, Su D, Stach E A, Ruoff R S. *Science*, 2011, 332: 1537

[36] Zhang K, Zhao Q, Tao Z, Chen J. *Nano Res*, 2013, 6: 38

[37] Zaragoza-Contreras E A, Hernndez-Escobar C A, Navarrete-Fontes A, Flores-Gallardo S G. *Micron*, 2011, 42: 263

[38] Ji X, Lee K T, Nazar L F. *Nat Mater*, 2009, 8: 500

[39] Kohlmeyer R R, Lor M, Deng J, Liu H, Chen J. *Carbon*, 2011, 49: 2352

[40] Sun B, Liu H, Munroe P, Ahn H, Wang G. *Nano Res*, 2012, 5: 460

[41] Cheng F, Shen J, Peng B, Pan Y, Tao Z, Chen J. *Nat Chem*, 2011, 3: 79

[42] Wang L, He X, Li J, Sun W, Gao J, Guo J, Jiang C. *Angew Chem Int Ed*, 2012, 51: 9034

[43] Zhu S, Zhou H, Hibino M, Honma I, Ichihara M. *Adv Funct Mater*, 2005, 15: 381

[44] Wu X, Jiang L, Cao F, Guo Y, Wan L. *Adv Mater*, 2009, 21: 2710

[45] Whittingham M S. *Chem Rev*, 2004, 104: 4271

[46] Goodenough J B, Kim Y. *Chem Mater*, 2009, 22: 587

[47] Ellis B L, Lee K T, Nazar L F. *Chem Mater*, 2010, 22: 691

[48] Cheng F, Liang J, Tao Z, Chen J. *Adv Mater*, 2011, 23: 1695

[49] Pivko M, Bele M, Tchernychova E, Logar N Z, Dominko R, Gaberscek M. *Chem Mater*, 2012, 24: 1041

[50] Wu Y, Wan C, Jiang C, Fang S, Jiang Y. *Carbon*, 1999, 37: 1901

[51] Zhang H, Tao H, Jiang Y, Jiao Z, Wu M, Zhao B. *J Power Sources*, 2010, 195: 2950

[52] Poizot P, Laruelle S, Grugeon S, Dupont L, Tarascon J M. *Nature*, 2000, 407: 496

[53] Chen J, Xu L N, Li W Y, Gou X L. *Adv Mater*, 2005, 17: 582

[54] Li W Y, Xu L N, Chen J. *Adv Funct Mater*, 2005, 15: 851

[55] Yoon T, Chae C, Sun Y K, Zhao X, Kung H H, Lee J K. *J Mater Chem*, 2011, 21: 17325

[56] Ji X, Herle P S, Rho Y, Nazar L F. *Chem Mater*, 2007, 19, 374

[57] Latorre-Sanchez M, Primo A, Garcia H. *J Mater Chem*, 2012, 22: 21373

[58] Li Z, Liu N, Wang X, Wang C, Qi Y, Yin L. *J Mater Chem*, 2012, 22: 16640

[59] Sun Y, Hu X, Luo W, Huang Y. *J Mater Chem*, 2012, 22: 19190

[60] Li H, Bai H, Tao Z, Chen J. *J Power Sources*, 2012, 217: 102

[61] Liu N, Wu H, McDowell M T, Yao Y, Wang C, Cui Y. *Nano Lett*, 2012, 12: 3315

[62] Jeong H M, Lee S Y, Shin W H, Kwon J H, Shakoor A, Hwang T H, Kim S Y, Kong B S, Seo J S, Lee Y M, Kang J K, Choi J W. *RSC Adv*, 2012, 2: 4311

[63] Fan J, Wang T, Yu C, Tu B, Jiang Z, Zhao D. *Adv Mater*, 2004, 16: 1432

[64] Zhao L, Hu Y, Li H, Wang Z, Chen L. *Adv Mater*, 2011, 23: 1385

[65] Borghols W J H, Wagemaker M, Lafont U, Kelder E M, Mulder F M. *J Am Chem Soc*, 2009, 131: 17786

[66] Shen L, Zhang X, Uchaker E, Yuan C, Cao G. *Adv Energy Mater*, 2012, 2: 691

[67] Padhi A K, Nanjundaswamy K S, Goodenough J B. *J Electrochem Soc*, 1997, 144: 1188

[68] Toprakci O, Toprakci H A K, Ji L, Xu G, Lin Z, Zhang X. *ACS Appl Mater Interfaces* 2012, 4: 1273

[69] Bai J, Gong Z, Lv D, Li Y, Zou H, Yang Y. *J Mater Chem*, 2012, 22: 12128

[70] Zhao L, Wang W, Wang A, Yu Z, Chen S, Yang Y. *J Electrochem Soc*, 2011, 158: A991

[71] Derrien G, Hassoun J, Panero S, Scrosati B. *Adv Mater*, 2007, 19: 2336

[72] Ji L, Rao M, Aloni S, Wang L, Cairns E J, Zhang Y. *Energy Environ Sci*, 2011, 4,: 5053

[73] Yin L, Wang J, Yu X, Monroe C W, NuLi Y, Yang J. *Chem Commun*, 2012, 48: 7868

[74] Lin Z, Liu Z, Fu W, Dudney N J, Liang C. *Adv Funct Mater*, 2012, 23: 1064

[75] Bruce P G, Freunberger S A, Hardwick L J, Tarascon J M. *Nat Mater*, 2012, 11: 19

[76] Wang L, Zhang T, Yang S, Cheng F, Liang J, Chen J. *J Energy Chem*, 2013, 22: 72

[77] Demir-Cakan R, Morcrette M, Nouar F, Davoisne C, Devic T, Gonbeau D, Dominko R, Serre C, Frey G, Tarascon J M. *J Am Chem Soc*, 2011, 133: 16154

[78] Li X, Cao Y, Qi W, Saraf L V, Xiao J, Nie Z, Mietek J, Zhang J G, Schwenzer B, Liu J. *J Mater Chem*, 2011, 21: 16603

[79] Liang C, Dudney N J, Howe J Y. *Chem Mater*, 2009, 21: 4724

[80] Elazari R, Salitra G, Garsuch A, Panchenko A, Aurbach D. *Adv Mater*, 2011, 23: 5641

[81] Jayaprakash N, Shen J, Moganty S S, Corona A, Archer L A. *Angew Chem Int Ed*, 2011, 50: 5904

[82] Qian J, Qiao D, Ai X, Cao Y, Yang H. *Chem Commun*, 2012, 48: 8931

[83] Cheng F, Chen J. *Chem Soc Rev*, 2012, 41: 2172

[84] Du J, Pan Y, Zhang T, Han X, Cheng F, Chen J. *J Mater Chem*, 2012, 22: 15812

[85] Shao Y, Liu J, Wang Y, Lin Y. *J Mater Chem*, 2009, 19: 46

[86] Zhang W, Sherrell P, Minett A I, Razal J M, Chen J. *Energy Environ Sci*, 2010, 3: 1286

[87] Dumitrescu I, Unwin P R, Macpherson J V. *Chem Commun*, 2009, 0: 6886

[88] Joo S H, Choi S J, Oh I, Kwak J, Liu Z, Terasaki O, Ryoo R. *Nature*, 2001, 412: 169

[89] Wang Y, Cheng L, Li F, Xiong H, Xia Y. *Chem Mater*, 2007, 19: 2095

[90] Liang Y, Wang H, Zhou J, Li Y, Wang J, Regier T, Dai H. *J Am Chem Soc*, 2012, 134: 3517

[91] Wang Z, Xu D, Xu J, Zhang L, Zhang X. *Adv Funct Mater*, 2012, 22: 3699